

# Optical properties of dental restorative materials in the wavelength range 400 to 700 nm for the simulation of color perception

Moritz Friebe  
Kirsten Povel  
Hans-Joachim Cappius  
Jürgen Helfmann

Laser- und Medizin-Technologie GmbH, Berlin  
Fabeckstrasse 60-62  
Berlin, 14195  
Germany

Martina Meinke

Charité—Universitätsmedizin Berlin  
Charité Campus Mitte  
Klinik für Dermatologie, Venerologie  
und Allergologie  
Center of Experimental and Applied Cutaneous  
Physiology  
Charitéplatz 1  
Berlin, 10117  
Germany

**Abstract.** Aesthetic restorations require dental restorative materials to have optical properties very similar to those of the teeth. A method is developed to this end to determine the optical parameters absorption coefficient  $\mu_a$ , scattering coefficient  $\mu_s$ , anisotropy factor  $g$ , and effective scattering coefficient  $\mu'_s$  of dental restorative materials. The method includes sample preparation and measurements of transmittance and reflectance in an integrating sphere spectrometer followed by inverse Monte Carlo simulations. Using this method the intrinsic optical parameters are determined for shade B2 of the light-activated composites TPH<sup>®</sup> Spectrum<sup>®</sup>, Esthet-X<sup>®</sup>, and theOrmocer<sup>®</sup> Definite<sup>®</sup> in the wavelength range 400 to 700 nm. By using the determined parameters  $\mu_a$ ,  $\mu_s$ , and  $g$  together with an appropriate phase function, the reflectance of samples with 1-mm layer thickness and shade B2 could be predicted with a very high degree of accuracy using a forward Monte Carlo simulation. The color perception was calculated from the simulated reflectance according to the CIELAB system. We initiate the compilation of a data pool of optical parameters that in the future will enable calculation models to be used as a basis for optimization of the optical approximation of the natural tooth, and the composition of new materials and their production process. © 2009 Society of Photo-Optical Instrumentation Engineers. [DOI: 10.1117/1.3250292]

Keywords: dental restorative material; aesthetic restoration; Monte Carlo simulation; optical parameter; absorption; scattering; color perception.

Paper 09101RR received Apr. 17, 2009; revised manuscript received Aug. 5, 2009; accepted for publication Aug. 11, 2009; published online Oct. 26, 2009.

## 1 Introduction

Dental restorative materials are used for the treatment of caries lesions. An aesthetic restoration should blend in with the tooth, i.e., there should be no visible difference between the restoration material and the treated tooth under all usual types of illumination. This includes all types of artificial light inside a building (lightbulbs, fluorescent lamps, LEDs) especially at the dental technician's workplace, flashlights (photographs), outdoor light (sun), and also filtered lighting, e.g., in the home garden. This goal can be reached only when the reflection spectra  $R(\lambda)$  of the restorative material and the tooth are the same in the detected/visible wavelength range. For this the optical properties  $\mu_a(\lambda)$ ,  $\mu_s(\lambda)$ , and  $g(\lambda)$  of the material must be at least similar to those of tooth tissue.

This requires that the optical properties of both the restorative material and natural teeth<sup>1</sup> are known and matched. In routine dentistry, failure to do this is still one of the most common reasons for having to replace restorations.<sup>2</sup>

Light-activated dental composites are the preferred direct filling materials for aesthetic, tooth-colored restorations. They

consist of a matrix with embedded filler particles of various kinds and size. Furthermore they contain several additives such as color pigments. Altogether this leads to a turbid optical appearance.

If other constraints are disregarded and the focus is on the optical appearance, the standard procedure used by manufacturers within the quality control process of dental composite filling materials is the measurement of diffuse reflectance spectra of samples of defined thickness (e.g., 1 mm). The measured data can be calculated on the basis of the  $L^*$ ,  $a^*$ ,  $b^*$  values following the CIELAB color system (Commission Internationale de l'Eclairage,  $L^*$ =brightness,  $a^*$ =chroma along red-green axis,  $b^*$ =chroma along yellow-blue axis), which enables comparison with color standards.

According to the radiation transport theory,<sup>3</sup> the "optical behavior" of turbid media can be described by the optical parameters absorption coefficient  $\mu_a(\lambda)$ , the scattering coefficient  $\mu_s(\lambda)$ , and the anisotropy factor  $g(\lambda)$ , together with an appropriate phase function. The scattering coefficient  $\mu_s(\lambda)$  of a turbid medium describes the probability of a light photon being scattered by a particle within this medium. The scattering phase function, often described by the parameter

Address all correspondence to: Hans-Joachim Cappius, Laser- und Medizin-Technologie GmbH, Berlin, Fabeckstrasse 60-62, Berlin, 14195 Germany. Tel: +49 30 8449 23 0; Fax: +49 30 8449 23 99; E-mail: h.cappius@LMTB.de.

**Table 1** Investigated composite resins and color shades.

Composite Resin/Manufacturer	Class of Composite	Shades (Vitapan Classical® Classification)
Spectrum/Dentsply DeTrey, Konstanz	hybrid composite	A1, A2, A3, A3.5, B1, B2, B3, C1, C2, C3
Esthet-X/Dentsply De Trey, Konstanz	hybrid composite	A1, A2, A3, A3.5, B1, B2, B3, C2, C3
Definite/Dentsply De Trey, Konstanz	ormocer	A1, A2, A3, A3.5, B2, C2

anisotropy factor  $g$ , provides information about the direction of the scattering. It gives a quantitative description of the probability for scattering in the direction of a certain angle. These optical parameters are intrinsic and do not depend on sample geometry and the arrangement of light source and detector. Intrinsic optical parameters cannot be measured directly but can be calculated from the measurable reflectance and transmission spectra by means of an inverse Monte Carlo simulation (iMCS). This is the most precise model to solve the light transport equation if complex boundary conditions prevent the use of analytical solutions.<sup>4-7</sup> The iMCS procedure has been proved to be successful for different tissues,<sup>8-10</sup> but has not yet been applied to dental composite materials, although it is possible to determine the CIELAB  $L^*$ ,  $a^*$ ,  $b^*$  color values of samples with a given thickness based on the optical parameters.

It was the aim of this study to compile a data pool of the optical parameters to extend the physical understanding of the optical properties of dental composites. By doing this it will enable the application of calculation models as a basis for optimization of the composition of new materials and their optical appearance. A method was developed for the sample preparation and the optical parameters of three different composite materials were determined in the visible wavelength range 400 to 700 nm. The comparison for different "VITA" shades of the material was categorized according to the VITAPAN classical® color scale, which is the most common color coding system for dental materials. The validity of the determined parameters is shown by a comparison of measured reflectance spectra of three samples of different material and arbitrary thickness with those predicted by simulation on the basis of the material dependent optical parameters and the given sample geometry. As an example of the application, a calculation method for determination and prediction of the color perception is presented and evaluated for a sample with a thickness of 1 mm, a black background, and the color shade B2, according to the CIELAB color system for given material thickness.

## 2 Materials and Methods

### 2.1 Dental Materials and Preparation Technique

Three different composite materials manufactured by Dentsply DeTrey (Konstanz, Germany) were investigated, each in the commonly available VITA shades shown in Table 1. The VITA classification system has letters A to D to

classify the groups of color appearance (e.g., yellowish). Within each group, numbers indicate decreasing brightness. The two hybrid composites, TPH Spectrum and Esthet-X, differ in composition with regard to their filler particles, and the ormocer Definite also has a different matrix material. For sample preparation, special preparation tools and a technique using ultrasound were developed to produce homogenous samples of adequate sample thickness and size, without air bubbles and with specular surfaces. For the spectrometric measurements, it was necessary to produce circular specimen disks each with a diameter of 22 mm for different sample thicknesses below 500  $\mu\text{m}$ . To optimize the measurability of transmission and reflectance spectra TPH Spectrum samples were prepared with a sample thickness of 400 and 250  $\mu\text{m}$  for Esthet-X samples and 200  $\mu\text{m}$  for Definite samples. Three samples were prepared for each shade making a total of 75 samples. For direct reflectance measurements  $R_{d,\text{meas}}$  TPH Spectrum, Esthet-X, and Definite samples of color shade B2 with a thickness of 1000  $\mu\text{m}$  were prepared. Samples were cured for 60 s in a laboratory VLC polymerization unit (Liculite, Dentsply DeTrey, Konstanz, Germany; VLC, visible light curing). The samples were stored in the dark and at room temperature for 24 h to enable them to be completely cured. Samples that showed inhomogeneities or air bubbles or had surface scratches were discarded.

### 2.2 Spectrometer Measurements

To determine the optical parameters, the diffuse reflectance  $R_d$ , the total transmission  $T_t$ , and the diffuse transmission  $T_d$  (excluding the collimated transmission and the diffuse transmission within an aperture of 5.3 deg) of the prepared material samples Spectrum, Esthet-X, and Definite were measured in the wavelength range from 400 to 700 nm in 5-nm steps by the integrating sphere technique using an UV/VIS/NIR spectrometer (Lambda 900, Perkin-Elmer Corporation, Norwalk, Connecticut USA). The measurement of  $T_d$  instead of the usually used collimated transmission allows measurement with only one integrating sphere. The experimental setup, described elsewhere,<sup>11,12</sup> enabled measurement of light transmission and reflectance with an error of less than 0.1%. To prove the validity of the simulated optical parameters and to compare the resulting color perception ( $R_{d,\text{sim}}$ ;  $L^*$ ,  $a^*$ ,  $b^*$ ), the diffuse reflectance  $R_d(\lambda)$  of the samples Spectrum, Esthet-X, and Definite in the color shade B2 were also measured ( $R_{d,\text{meas}}$ ) for the sample thickness 1000  $\mu\text{m}$ .

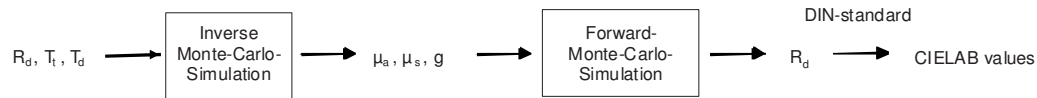


Fig. 1 Scheme of the determination of the color perception based on the optical parameters.

### 2.3 Monte Carlo Simulation

A specially developed iMCS simulation program was used that also takes into account the geometry of the optical setup and all radiation losses. Simulations with more than  $10^6$  photon trajectories for each wavelength were calculated leading to statistical errors of less than 0.15%. Typical standard deviations of three determinations of  $\mu_a$ ,  $\mu_s$ , and  $1-g$  were in the range 3 to 5%. The iMCS used an estimated set of start parameters  $\mu_a$ ,  $\mu_s$ , and  $g$  from the Kubelka-Munk theory to calculate the resulting values  $R_d$ ,  $T_t$ , and  $T_d$  for each wavelength. These were then compared with the experimentally measured  $R_d$ ,  $T_t$ , and  $T_d$  values at the same wavelength. By systematic variation of  $\mu_a$ ,  $\mu_s$ , and  $g$ , deviation of the simulated  $R_d$ ,  $T_t$ , and  $T_d$  values from the measured ones was minimized until a set of optical parameters were found where the deviations were within the error threshold. Repeating this procedure wavelength by wavelength at 5-nm increments, each within the spectral range of interest leads to a spectrum of  $\mu_a(\lambda)$ ,  $\mu_s(\lambda)$ , and  $g(\lambda)$ . Due to the high sensitivity of the simulation, it was possible to fit an adaptable phase function.<sup>8,13</sup> Scattering phase functions that do not describe realistic scattering processes do not enable successful simulations within the error tolerances. The type and parameters of the phase function can be determined by minimizing the error tolerances. These presimulations showed that the Henyey-Greenstein phase function<sup>4</sup> was best suited for iMCS of the two hybrid composites, whereas the Reynolds-McCormick phase function<sup>7</sup> (with an  $\alpha$  factor of 1.5) was best suited for the ormocer. To increase the precision of the simulation, the absorption coefficients  $\mu_a(\lambda)$ , determined on samples with a thickness of between 200 and 400  $\mu\text{m}$  (material dependent, see Sec. 2.1), were corrected with measurements of composite samples with 5-mm thickness and a modified iMCS determination of  $\mu_a(\lambda)$ , keeping  $\mu_s(\lambda)$  and  $g(\lambda)$  at predetermined values for the thin samples.

The wavelength-dependent refractive index of the material is an important input parameter for the simulation as it primarily influences the reflection at interfaces<sup>5,14</sup> and therefore the precision of the simulation. As there is very little information available about the refractive index of dental composites, refractive indices of each composite were determined from 400 to 700 nm using an Abbe refractometer. The samples were molded on an optical glass surface to minimize errors due to surface roughness.

### 2.4 Determination of the Color Perception Following the CIELAB System

Based on the determined  $\mu_a$ ,  $\mu_s$ , and  $g$  values, the diffuse reflectance values  $R_d$  for a sample of Esthet-X, Spectrum, and Definite with an arbitrary color shade and thickness (in this case B2 and 1 mm) were calculated using a forward Monte Carlo simulation program. Based on the material-dependent simulated reflectance spectra  $R_{d,\text{sim}}$ , the X, Y, and Z standard

color values were calculated according to DIN standard 5033 (Ref. 15) in 10-nm steps in the range 400 to 700 nm, with respect to the standard light source D65 and the 2-deg standard observer, and transformed to the  $L^*$ ,  $a^*$ ,  $b^*$  values according to the CIELAB system. Figure 1 shows the principle of the procedure used.

The determination of the  $L^*$ ,  $a^*$ ,  $b^*$  values was repeated for samples with a thickness of 1 mm and color shade B2 based on measured reflectance spectra. All measured and calculated CIELAB values assume a black background. To compare the CIELAB values of the simulated reflectance spectra with those of the measured ones, color differences  $\Delta E_{ab}^*$  were determined between measured and predicted values in accordance with Eq. (1) (DIN standard 6174)<sup>16</sup>:

$$\Delta E_{ab}^* = [(\Delta L^*)^2 + (\Delta a^*)^2 + (\Delta b^*)^2]^{1/2}, \quad (1)$$

with  $\Delta L^*$  as the difference between  $L^*_{\text{sample}}$  and  $L^*_{\text{reference}}$ ,  $\Delta a^*$ , and  $\Delta b^*$  analogous.

## 3 Results and Discussion

### 3.1 Determination of the Optical Parameters

Applying the iMCS, in contrast to the Kubelka-Munk method, enables a separation of optical properties into the optical parameters absorption and scattering coefficient with high precision.<sup>4</sup> Figure 2 shows the results of the iMCS, i.e., the optical parameters  $\mu_a(\lambda)$ ,  $\mu_s(\lambda)$ ,  $g(\lambda)$ , and  $\mu'_s(\lambda)$  [ $=\mu_s(1-g)$ ] dependent on the wavelength, as for example, for the color shade B2 for all three composite resins.

The maximum absorption at 400 nm is 0.38  $\text{mm}^{-1}$  for Esthet-X, 0.32  $\text{mm}^{-1}$  for Spectrum, and 0.17  $\text{mm}^{-1}$  for Definite. All absorption values decrease below 0.03  $\text{mm}^{-1}$  at 700 nm, leading to the perception of a yellowish color. The ormocer Definite shows the highest  $\mu_s(\lambda)$  of 26  $\text{mm}^{-1}$  at 400 nm and decreases continuously to values about 14  $\text{mm}^{-1}$  at 700 nm. The scattering coefficient of Spectrum decreases from 8 to 5  $\text{mm}^{-1}$  within the observed wavelength range. Esthet-X shows  $\mu_s(\lambda)$  of 19  $\text{mm}^{-1}$  at 400 nm decreasing more distinctly than Spectrum to 4  $\text{mm}^{-1}$  at 700 nm. The anisotropy factor  $g(\lambda)$  shows a strong forward scattering of Esthet-X and Definite with values of about 0.8 over the whole spectral range. Definite exhibits extreme forward scattering with values above 0.95 leading to the lowest effective scattering coefficient  $\mu'_s(\lambda)$  with values between 1.0 and 0.7  $\text{mm}^{-1}$ . Esthet-X shows the highest effective scattering with values above 3  $\text{mm}^{-1}$  at 400 nm, whereas Spectrum and Definite are lower, with values of 1.8 and 1.0  $\text{mm}^{-1}$  at 400 nm. The effective scattering of all three resins decreases with wavelength converging to values in the range 0.6 to 0.8 at 700 nm.

Figure 3 shows the absorption coefficient depending on wavelength for Esthet-X in 10 different shades according to the VITAPAN classical<sup>®</sup> system. At 400 nm,  $\mu_a(\lambda)$  shows

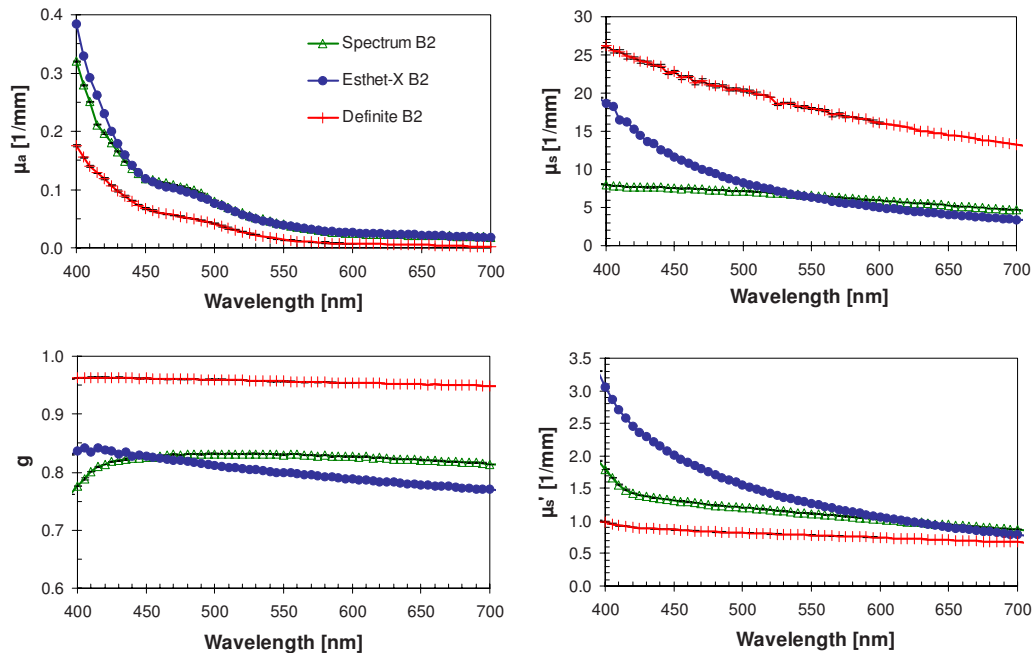


Fig. 2 Wavelength-dependent comparison of optical parameters of the three composite resins for shade B2.

values in the range 0.4 to 0.6 mm<sup>-1</sup> depending on the shades A1 to C3, whereas at 700 nm, the range decreases to values below 0.05 mm<sup>-1</sup>. Scattering coefficient  $\mu_s(\lambda)$ , anisotropy factor  $g(\lambda)$ , and effective scattering coefficient  $\mu'_s(\lambda)$  show no significant dependency on the color shades (not shown).

The decrease of absorption [ $\mu_a(\lambda)$ ] and effective scattering [ $\mu'_s(\lambda)$ ] of all three composite resins with increasing wavelengths is in agreement with the results of other studies which use the Kubelka-Munk method.<sup>14,17</sup> Furthermore, the results support statements made by other authors that absorption takes place in the color pigments or matrix<sup>14</sup> and scattering is mainly due to the filler particles.<sup>17</sup> There are more differences in  $\mu_a(\lambda)$  of the hybrid composites Spectrum and Esthet-X compared to the ormocer Definite than between Spectrum and Esthet-X which have the same matrix (Fig. 2). Scattering coefficient  $\mu'_s(\lambda)$ , anisotropy factor  $g(\lambda)$ , and reduced scattering coefficient  $\mu'_s(\lambda)$  are less dependent on shades (data not shown), but differ greatly between the three materials, each containing different filler particles (Fig. 2).

Scattering is more influenced by different sizes and the kinds of filler particles than by the color pigments, the opposite being true for absorption. At short wavelengths from 400 to 500 nm, i.e., the blue part of visible light, Esthet-X shows a steeper curve for the scattering coefficient  $\mu_s(\lambda)$ . From this it can be deduced that for the filler particle size distribution of the materials, Esthet-X contains a larger portion of small filler particles with dimensions relating to the blue wavelength range than the other two composites Spectrum and Definite. The shades of the composite materials were adjusted by the addition of color pigments, e.g., metal oxides. Within the investigated VITA color shades A to C, the degree of brightness is given by the shade numerals 1 to 3 (3.5), guided mainly by the concentration of color pigments. Shades A4, B4, and C4 as well as the range D2 to D4 were not investigated. In support of this, a strong correlation was

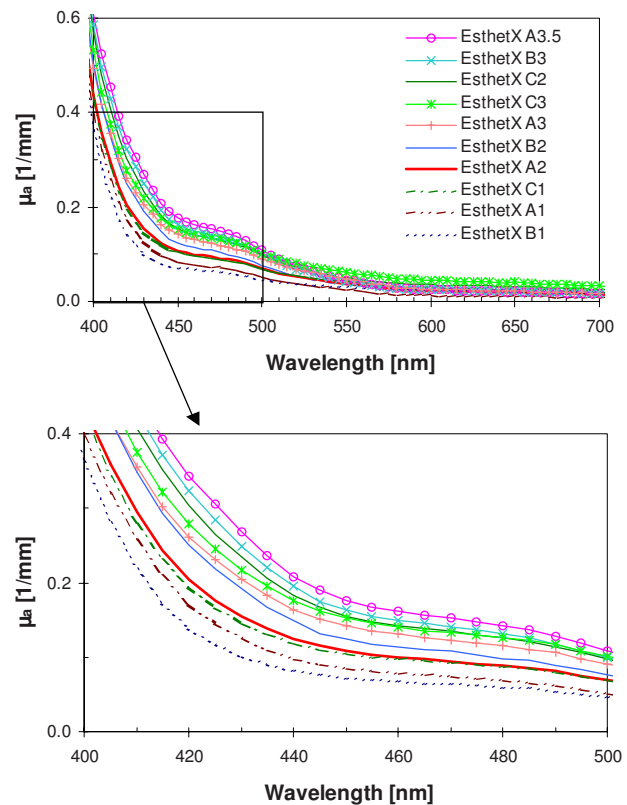
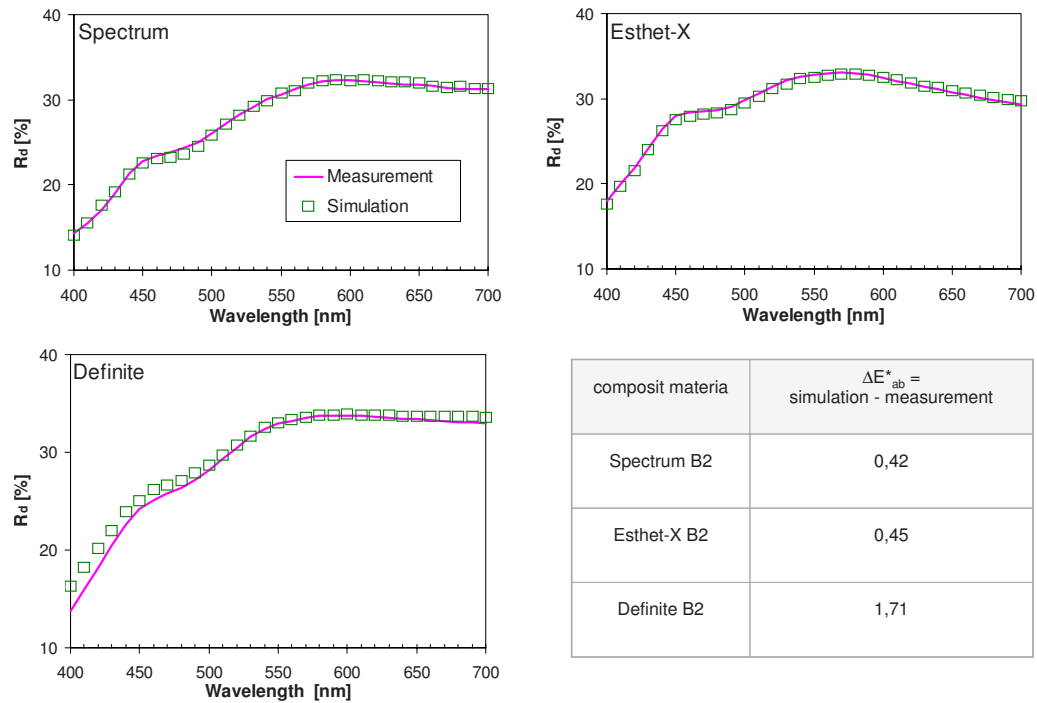


Fig. 3 Absorption coefficient  $\mu_a$  of Esthet-X for different shades dependent on the wavelength.





**Fig. 4** Comparison of the measured and simulated  $R_d$  values of the different composites for shade B2 and a sample thickness of approx. 1 mm; Table: Calculated color difference  $\Delta E_{ab}^*$  between simulation and measurement. (Color online only.)

found at 450 nm for the shade numerals and the absorption coefficient  $\mu_a(\lambda)$  after running rank correlation according to Spearman.

The maximum lightness for shade numeral 1 (i.e., A1, B1 and C1) shows the lowest values for the absorption coefficient  $\mu_a(\lambda)$ , focusing on the area of short wavelengths (Fig. 3). The situation changes for longer wavelengths. There was only a low correlation for shade numerals at 660 nm and a high correlation for shade letters (color groups). Statistical analysis using the H-test, according to Kruskal und Wallis, showed that significant differentiation of shades with  $p < 0.05$  is possible at 450 and 660 nm for all optical parameters, except for  $\mu_s(\lambda)$  of Definite at 450 nm. Shade numerals within one shade letter could be significantly differentiated for the absorption coefficient  $\mu_a(\lambda)$  at 450 nm for all materials, with the exception of C1 to C3 of Esthet-X. There was no significant differentiation at 450 nm for the shade letters.

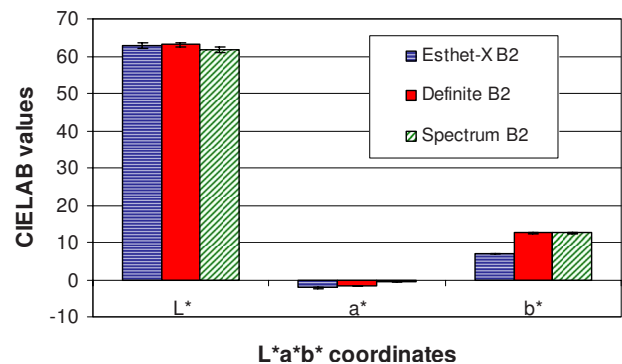
### 3.2 Comparison of the Reflectance Spectra

Figure 4 shows a comparison of the simulated and measured wavelength dependent diffuse reflectance  $R_d(\lambda)$  for one sample with a thickness of approx. 1 mm and color B2 for each of Esthet-X ( $d=1092 \mu\text{m}$ ), Spectrum ( $d=1099 \mu\text{m}$ ), and Definite ( $d=1032 \mu\text{m}$ ). The  $R_d(\lambda)$  value was directly measured as well as determined by simulation using the forward MCS on the basis of the optical parameters  $\mu_a(\lambda)$ ,  $\mu_s(\lambda)$ , and  $g(\lambda)$  using the iMCS and the thickness of the directly measured samples. The comparison shows very good agreement between calculated and measured diffuse reflectance data  $R_d(\lambda)$ . This is also valid for Definite, which shows minimal deviations only at short wavelengths. This result indicates the validity of the determined material dependent

optical parameters  $\mu_a(\lambda)$ ,  $\mu_s(\lambda)$ , and  $g(\lambda)$ , enabling a valid prediction of the reflectance spectra of a sample of arbitrary thickness and geometry.

### 3.3 Determination of the Color Perception Following the CIELAB System

According to Sec. 2.4, the CIELAB values  $\Delta L^*$ ,  $\Delta a^*$ , and  $\Delta b^*$  can be calculated from simulated or measured  $R_d$  values to compare different materials or shades. As an example, Fig. 5 shows the comparison of the calculated CIELAB values for the composite materials Esthet-X, Spectrum and Definite for shade B2 with a 1-mm sample thickness based on the simulated  $R_d$  spectra. Perceptible color differences were found between the investigated composites, which were especially large between Esthet-X and Spectrum, as well as between Definite and Esthet-X. Only Spectrum and Definite



**Fig. 5** CIELAB values of the coordinates  $L^*$ ,  $a^*$ , and  $b^*$  for three different composite materials.

**Table 2** The  $\Delta L^*$ ,  $\Delta a^*$ , and  $\Delta b^*$  color perception and color differences  $\Delta E_{ab}^*$  of shade B2 using a 1-mm sample thickness for standard light D65 and a 2-deg standard observer.

CIELAB at 1 mm	Esthet-X to Spectrum	Esthet-X to Definite	Definite to Spectrum
$\Delta L^*/$ color perception	1.15/lighter	-0.25/darker	1.40/lighter
$\Delta a^*/$ color perception	-1.64/more green	-0.64/more green	-1.00/more green
$\Delta b^*/$ color perception	-5.48/more blue	-5.48/more blue	0.00/the same
$\Delta E_{ab}^*$	5.82	5.51	1.72

exhibited values with  $\Delta E_{ab}^* < 2$ , which is defined as clinically undistinguishable.<sup>18</sup> In general, Esthet-X had a more bluish hue. The exact values for the differences of CIELAB values  $\Delta L^*$ ,  $\Delta a^*$ , and  $\Delta b^*$ , the resulting color perception and the calculated color differences  $\Delta E_{ab}^*$  are given in Table 2.

Furthermore, the CIELAB values can be used to compare the perceptible color difference between simulated and measured reflectance spectra. This has been done for the simulated and directly measured  $R_d$  spectra shown in Fig. 4. The table in Fig. 4 shows the respective  $L^*$ ,  $a^*$ , and  $b^*$  differences. The calculated color differences show values of  $\Delta E_{ab}^* < 0.5$  for the hybrid resin composites, which is defined as not visible for 50% of observers.<sup>18</sup> Definite exhibits an  $\Delta E_{ab}^*$  value of 1.71, which is within the clinically acceptable range of  $\Delta E_{ab}^* < 2$ . Grajower et al.<sup>17</sup> used the Kubelka-Munk method to achieve a lower simulation precision with higher  $\Delta E_{ab}^*$  deviations in the range of moderate perceptibility ( $\Delta E_{ab}^* = 1.72$  to 4.58). Ikeda et al.<sup>19</sup> also found perceptible color differences with  $\Delta E_{ab}^*$  values from 1.7 to 7.4.

## 4 Conclusion

A better physical understanding of the optical properties of dental composites was achieved. Also a start was made to compile a data pool for the optical parameters  $\mu_a(\lambda)$ ,  $\mu_s(\lambda)$ , and  $g(\lambda)$  in the visible wavelength range 400 to 700 nm of the three dental composites Esthet-X, Spectrum, and Definite for different VITA shades. A combination of the presented methods, including sample preparation, measurement, and simulation, led to a more precise determination of optical properties than the more commonly used Kubelka-Munk method.<sup>14,17,20</sup>

The procedure presented here enables the precise prediction of the diffuse reflectance spectrum of a sample of arbitrary thickness and geometry using knowledge of the optical parameters  $\mu_a(\lambda)$ ,  $\mu_s(\lambda)$ , and  $g(\lambda)$ . The (simulated) diffuse reflectance  $R_d$  is the essential optical parameter for the comparison of color perception, independent of the light source.

A calculation method was presented, as an example of application, for the determination and prediction of the color perception according to the CIELAB color system from a simulated  $R_d$ . Based on the simulation determined optical parameters  $\mu_a(\lambda)$ ,  $\mu_s(\lambda)$ , and  $g(\lambda)$ , which are independent of the sample thickness, the reflectance for samples of a 1-mm layer thickness and color B2 could be predicted using the forward Monte Carlo simulation with a high degree of agreement compared to the measured data.

Precise calculation of the color perception from the simulated reflectance spectra could be used, for example, to predict the influence of the layer thickness or variations of sample shape on the observed color shade.

After the investigation of composites, the next step will be to determine the optical parameters of ceramics and human teeth to directly compare the optical properties of artificial restoration materials with natural teeth. Finally, the presented investigation could be advantageous in the field of laser application, providing more detailed knowledge about laser processing and ablation of dental and other polymers. In the future, the determination of optical parameters could be used to influence and control the development of new dental restorative materials by comparing experimental material compositions with existing ones or alternatively with the optical properties of teeth. Furthermore, more information about the absorption and scattering characteristics of the base materials used for composites, i.e., filler, matrix material and color pigments, is required. This could be used to form the basis of a procedure to optimize the composition of new materials and their production process or quality control.

## Acknowledgments

The authors would like to acknowledge Dentsply DeTrey, Konstanz, Germany, for supplying composite restorative materials and the visible light curing (VLC) polymerization unit.

## References

1. D. Spitzer and J. J. ten Bosch, "The absorption and scattering of light in bovine and human dental enamel," *Calcif. Tiss. Res.* **17**, 129–137 (1975).
2. N. H. Wilson, F. J. Burke, and I. A. Mjor, "Reasons for placement and replacement of restorations of direct restorative materials by a selected group of practitioners in the United Kingdom," *Quintessence Int.* **28**, 245–248 (1997).
3. S. Chandrasekhar, *Radiative Transfer*, Dover Publications, New York (1960).
4. A. Roggan, "Dosimetrie thermischer Laseranwendungen in der Medizin. Untersuchung der optischen Gewebeigenschaften und physikalisch-mathematische Modellentwicklung," Dissertation, TU Berlin, *Fortschritte in der Lasermedizin* **16**, G. Müller, H. P. Berlien Eds., Ecomed, Landsberg (1997).
5. A. Roggan, H. Albrecht, K. Dörschel, O. Minet, and G. Müller, "Experimental set-up and Monte-Carlo model for the determination of optical properties in the wavelength range 330–1100 nm," *Proc. SPIE* **2323**, 21–36 (1995).
6. M. Hammer, A. Roggan, D. Schweitzer, and G. Müller, "Optical properties of ocular fundus tissue—an *in vitro* study using double integrating sphere technique," *Phys. Med. Biol.* **40**, 963–978 (1995).
7. A. Roggan, M. Friebel, K. Dörschel, A. Hahn, and G. Müller, "Optical properties of circulating human blood in the wavelength range

- 400–2500 nm,” *J. Biomed. Opt.* **4**, 36–46 (1999).
8. M. Friebel, A. Roggan, G. Müller, and M. Meinke, “Determination of optical properties of human blood in the spectral range 250–1100 nm using Monte Carlo simulations with hematocrit-dependent effective scattering phase functions,” *J. Biomed. Opt.* **11**(3), 031021 (2006).
  9. A. Roggan, K. Dörschel, O. Minet, D. Wolff, and G. Müller, “The optical properties of biological tissues in the near-infrared wavelength range: review and measurements,” in *Laser-Induced Interstitial Thermotherapy*, G. Müller and A. Roggan, Eds., pp. 10–44, SPIE Press, Bellingham, WA (1995).
  10. A. Kienle and R. Steiner, “Determination of the optical properties of tissue by spatially resolved transmission measurements and Monte Carlo calculations,” *Proc. SPIE* **2077**, 142–152 (1994).
  11. K. Weniger, “Optische Eigenschaften von dentalen Kompositfüllungsmaterialien,” Dissertation, Charité-Universitätsmedizin Berlin, in Müller G. (Hrsg.): Forschungsberichte 3 / Laser- und Medizintechnologie Berlin, dissertation. de—Verlag im Internet GmbH, Berlin (2004).
  12. M. Meinke, I. Gersonde, M. Friebel, J. Helfmann, and G. Müller, “Chemometric determination of blood parameters using VIS-NIR spectra,” *Appl. Spectrosc.* **59**(6), 826–835 (2005).
  13. A. Kienle, F. K. Forster, and R. Hibst, “Influence of the phase function on the determination of the optical properties of biological media,” *Proc. SPIE* **4432**, 40–47 (2001).
  14. C. L. Yeh, Y. Miyagawa, and J. M. Powers, “Optical properties of composites of selected shades,” *J. Dent. Res.* **61**, 797–780 (1982).
  15. Deutsches Institut für Normung e.V., DIN-Norm 5033, Farbmessung Teil 1 bis 9, Beuth-Verlag, Berlin (1979–1992) [in German].
  16. Deutsches Institut für Normung e.V., DIN-Norm 6174, Farbmessung Bestimmung von Farbabständen bei Körperfarben nach der CIELAB-Formel, Beuth-Verlag, Berlin (1979) [in German].
  17. R. Grajower, W. T. Wozniak, and J. M. Lindsay, “Optical properties of composite resin,” *J. Oral Rehabil.* **9**, 389–399 (1982).
  18. R. D. Paravina, *Instrumental Color Matching Methods in Dentistry*, Zadužbina Anđejević, Beograd (1999).
  19. T. Ikeda, A. Nakanishi, T. Yamamoto, and H. Sano, “Color differences and color changes in vita shade tooth-colored restorative materials,” *Am. J. Dent.* **16**(6), 381–384 (2003).
  20. M. Taira, M. Okazaki, and J. Takahashi, “Studies on optical properties of two commercial visible-light-cured composite resins by diffuse reflectance measurements,” *J. Oral Rehabil.* **26**, 329–337 (1999).